APPENDIX D

THE PHYSICAL STRUCTURE OF VIRUSES AND BACTERIA, WHICH MAKE THEM EXTREMELY SUSCEPTIBLE TO DESTRUCTION BY SPECIFIC STRUCTURAL RESONANT MECHANICAL VIBRATIONS

In Appendix A it was shown how Dr. Royal Raymond Rife was able in 1920 to build the first of five optical microscopes, which were able to overcome the normally found Fraunhofer diffraction limitations to size resolution occurring in today's commonly used optical microscopes. Rife's microscopes were able to see viruses. In Appendix B it was shown how Rife , while observing with his microscope, used his frequency instrument to destroy viruses and bacteria. It was also alluded to it being some sort of resonant vibrations set up in the microbe structure by the frequency instrument that destroyed the microbe. In Appendix C an example of a simple virus capsid (protein coat) was used to show how structural resonance vibrations can destroy a virus. In this Appendix D a detailed look at the physical structure of virus capsids will show that they have construction which is particularly susceptible to destruction by structural resonant vibrations. Also a look at bacteria cell membrane and bacteria cell wall structure will suggest how and why bacteria are also susceptible to destruction by exposure to structural resonant vibrations.

PLEASE COPY AND SHARE

The study of virus types and structure is a very complex endeavor. In this Appendix we will only consider simple virus capsid structures in detail. However, these simple virus capsid structures will have structure patterns which are common to all viruses and will illustrate why all viruses are susceptible to destruction by structural resonant vibrations. Almost all viruses of interest can be classified under two headings: 1) Viruses with helical symmetry, and 2) Viruses with icosahedral symmetry.

Two viruses with helical symmetry are illustrated in Figures 1 and 2 and will serve as prototypes of the viruses of helical symmetry. Figure 1 illustrates a segment of the well known tobacco mosaic virus. In this virus, identical protein molecules associate with the virus RNA genome to form a right handed helix pattern as shown. This assembled virus is also called a naked helical nucleocapsid. Naked because there is no lipid bilayer coat around the helical nucleocapsid. When ever the genome of a virus is enclosed by a protein coat it is called a nucleocapsid. Figure 2 illustrates a helical nucleocapsid strand which has been wound into a still much larger helix, which is encapsulated in a lipid bilayer envelop membrane, which has glycoprotein spikes on its outer surface. The tobacco mosaic virus structure is typical of many viruses that cause plant diseases. The virus structure illustrated in Figure 2 is typical of many viruses that cause animal/human diseases. For example, influenza and measles viruses. We will see later on in this appendix that viruses with helical symmetry can be treated as torsional oscillators and by over driving these torsional oscillators at their resonant frequency they can be destroyed. However, first we will study the protein coat (capsid) structure of the by far most common and numerous types of viruses to cause diseases in plants and animals. Namely, viruses with icosahedral symmetry.

Illustrated in Figure 3A,B, and C are three different views of a icosahedron. The icosahedron has 20 equilateral triangle faces, 12 vertices, and 30 edges. The opposing vertices lay on an axis of five fold symmetry as illustrated in Figure 3A. In other words

each time the icosahedron is rotated ($72^0 = 360^0/5$) about one of these six axes it is brought back into the same state. The axes through the centers of opposing equilateral triangles have 3-fold symmetry as illustrated in Figure 3B. In other words each time the icosahedron is rotated ($120^0 = 360^0/3$) about one of these 10 axes it is brought back into the same state. The 15 axes through the centers of opposing edges are axes of 2-fold symmetry, as illustrated in Figure 3C. In other words each time the icosahedron is rotated ($180^0 = 360^0/2$) about one of these 15 axes it is brought back into the same state. Figure 4A and B illustrate how a section of an isometric net can be folded into an icosahedron. Such an isometric net for constructing icosahedrons is illustrated in Figure 5. Figure 5A shows the isometric net section of Figure 4A. Now it is an amazing fact that most viruses have capsids surrounding the viral genome, which have icosahedral symmetry. It is this fact of icosahedral symmetry of the capsid that allows us to associate a repeating protein pattern with the specific isometric net illustrated in Figure 5, from which a virus capsid can be constructed by the method illustrated in Figure 4A. The circles in Figures 5B,C,D,E, and F represent protein molecules. You can imagine isometric nets in which each of the protein molecule patterns of Figures 5B,C,D,E, and F each fill the entire isometric net. Then by removing an isometric net segment as illustrated in Figure 5A from each of these isometric nets, five different virus capsids can be constructed. It should be noted that even though I have shown identical circles implying identical protein molecules in each of the isometric nets, in fact most viruses use two or more different protein molecules in their capsid. So just think of the circles as place holders for different protein molecules.

Do to the high symmetry of the specific isometric net of Figure 5, which produces icosahedral symmetry, it is possible to chose isometric net sections, which have the same shape and symmetry as the isometric net section of Figure 5A, but consists of integer multiples of the 20 unit triangles of Figure 5A. These larger isometric net sections can of course also be folded into an icosahedral shape, but are properly called deltahedra. Some of these possible deltahedrals are illustrated in Figure 6. Figure 7 illustrates some of the possible equilateral triangular deltahedral faces, some of which were illustrated in Figure 6. For a simple concrete example consider Figure 8. In Figure 8 we have constructed an isometric net as was suggested in Figure 5C. In Figure 8, three equilateral triangular (protein) faces are illustrated, namely triangles ABE, ACF, and ADG. These triangle faces are illustrated in virus capsid models you are going to construct, from Figures 9A,9B, and 9C respectfully. These are all simple examples of deltahedrals illustrated in Figure 6A. Now looking back at Figures 3D,E, and F we see spherical or inflated versions of Figures 3A,B, and C respectively. The inflated versions have the exact same 5,3,2 rotational symmetry as the icosahedra and can be constructed from the same stretched or deformed isometric net as the icosahedra was. The importance of this is that viruses with icosahedral symmetry are generally spherical in living tissue due to hydrophilic interaction between virus coat proteins and or lipid bilayer with tissue water and osmotic pressure.

Figures 9A,B,C,D,E,F,G, and H are all simple virus capsids for you to construct. The importance in constructing these capsid models is, that until you construct them, you are not likely to clearly see just how highly symmetric , over lapping, and closed on its self these periodic protein clump patterns on virus capsids are. The importance of this high symmetry, over lapping, and closed on its self periodicity is that it makes each virus type

FIGURE 1

TABACCO MOSAIC VIRUS

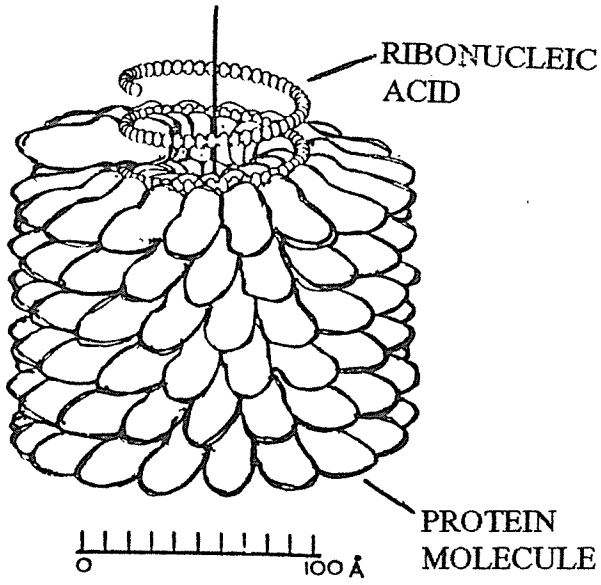

FIGURE 2

ENVELOPED HELICAL VIRUS

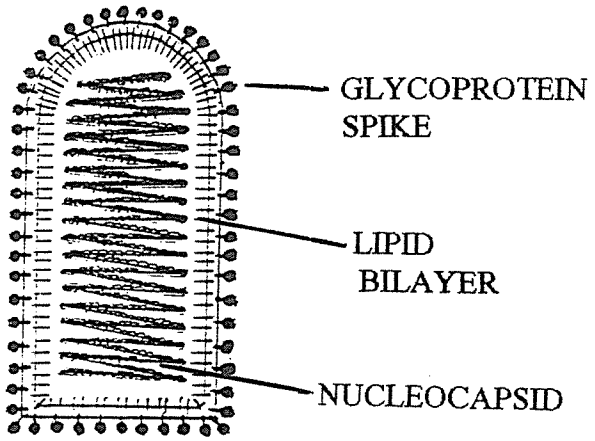

FIGURE 3

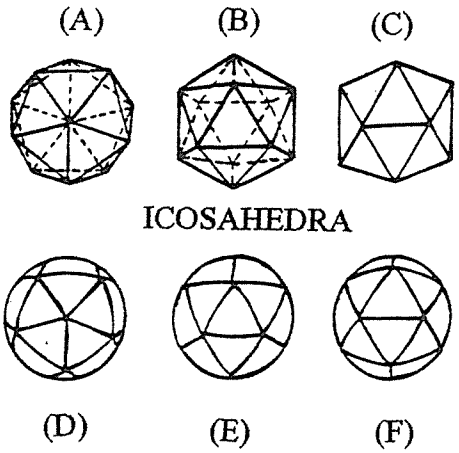

FIGURE 4

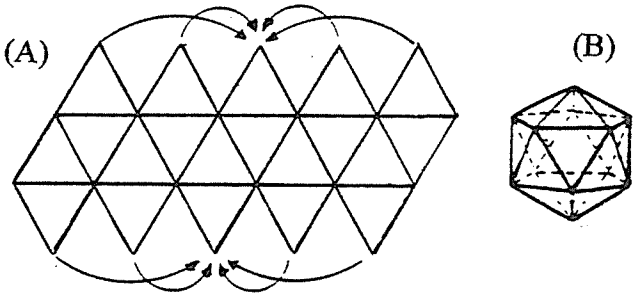

FIGURE 5

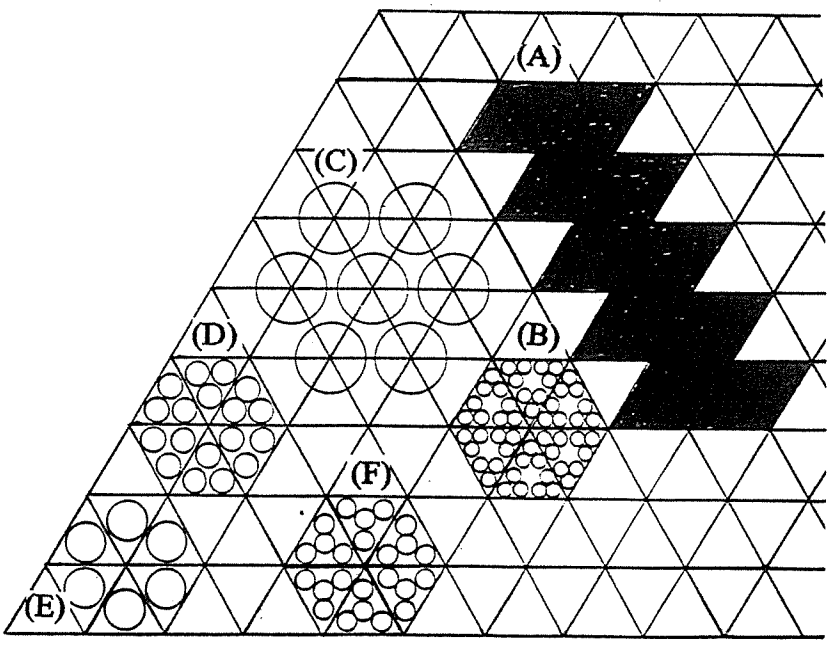

FIGURE 6

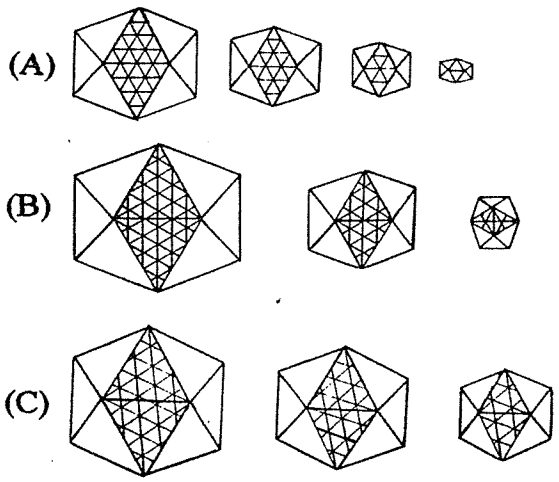

FIGURE 7

ILLUSTRATING ISOLATERAL FACES OF DELTAHEDRA ON AN ISOMETRIC NET

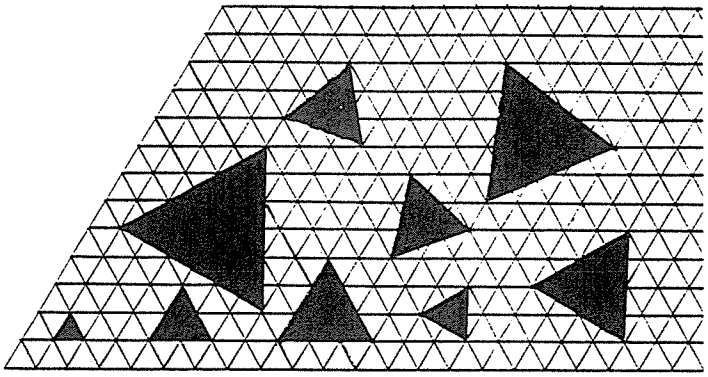

FIGURE 8

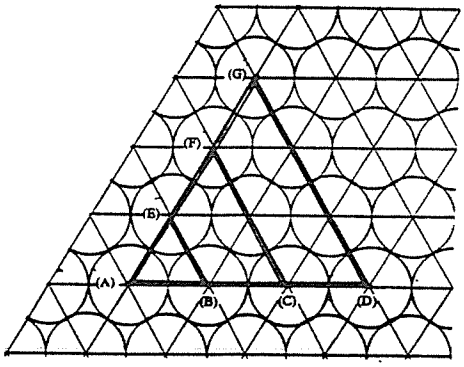

FIGURES 9A - H

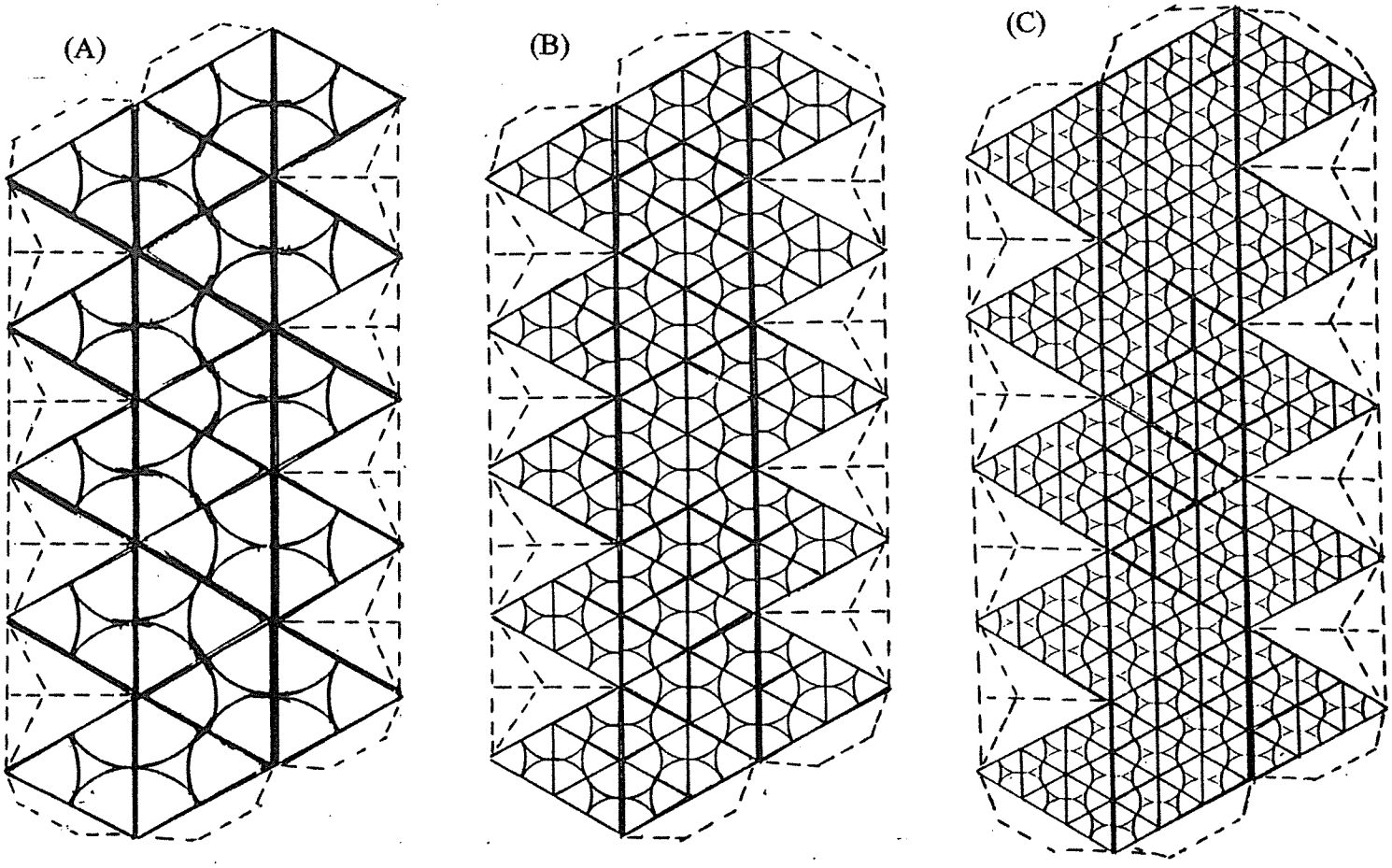

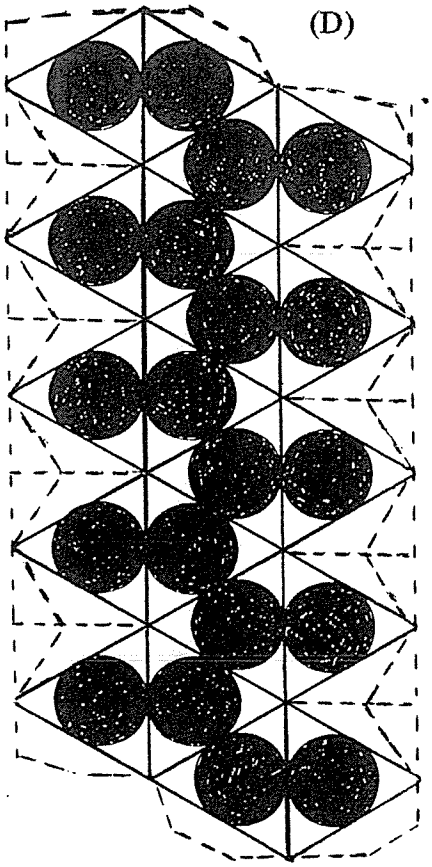

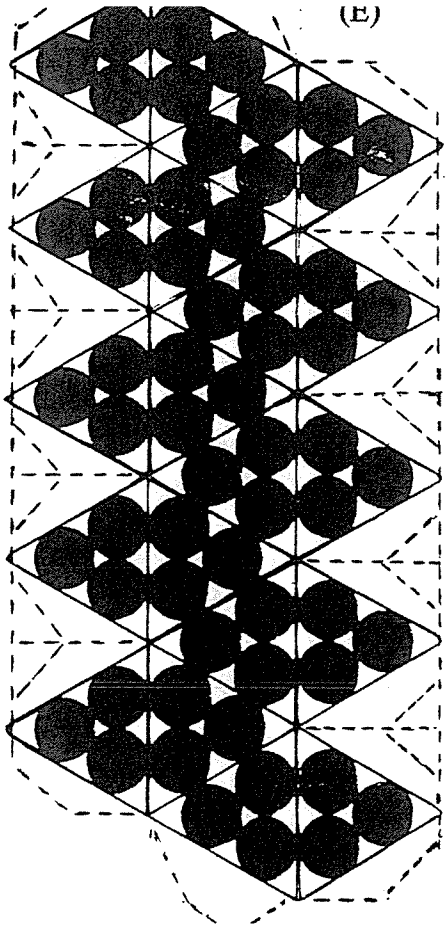

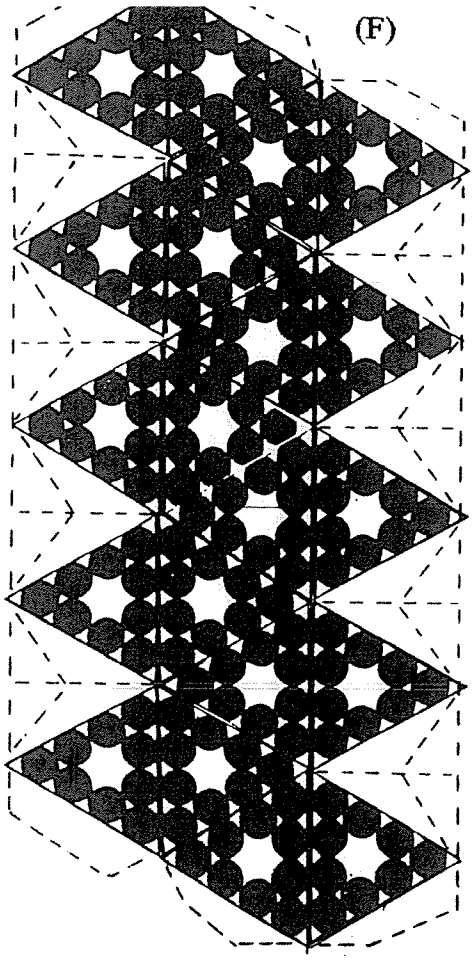

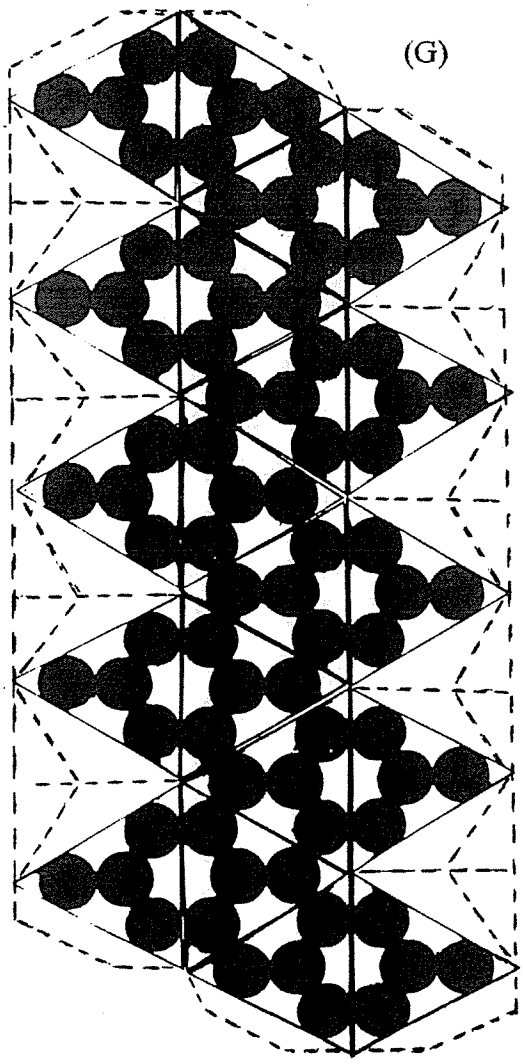

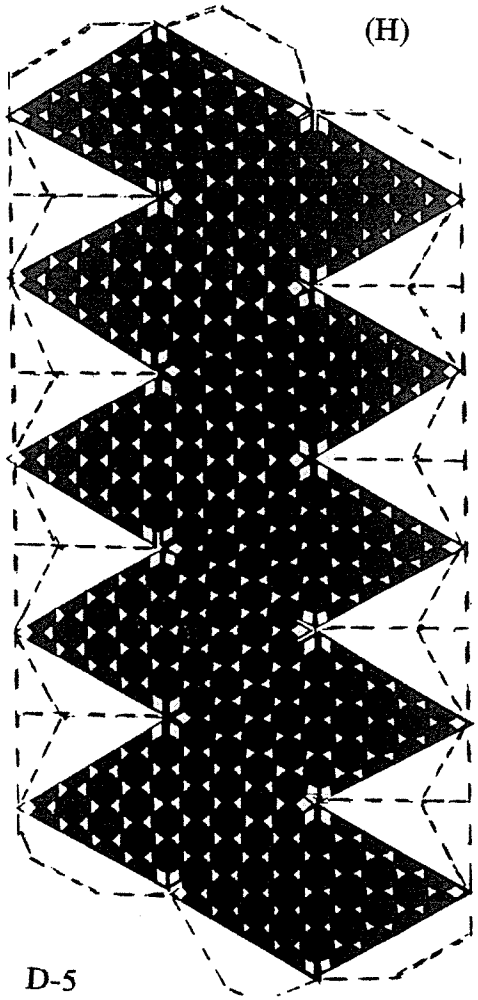

FIGURE 10

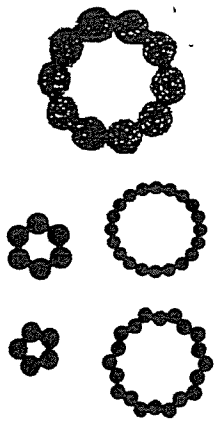

exceedingly easy to destroy with its own specific frequencies of mechanical structural resonance vibrations.

Here are the instructions for assembly of the virus coat in Figures 9A,B,C,D,E,F,G, and H. First go to a copy machine and enlarge the figure 122% two times. This will give almost a page full of virus coat. Second, make another copy of the last enlargement onto thick cardboard copy paper. You may have to look around to find the right copy machine for this. Third, cut out all dashed lines on the cardboard copy. You should now have something that looks like Figure 4A except for extra tabs for gluing the model together. (I have found that Elmer's Glue All works well). Fourth , taking a straight edge ruler and lining its edge up congruent with all of the equilateral triangle facet edges as those shown in Figure 4A, fold the cardboard over the ruler edge until a 90 degree fold angle is achieved, while folding away from the faces shown in Figures 9A through 9H. Be sure to fold all of the glue tabs this way also. Fifth, begin gluing adjacent tabs flush together. It may prove helpful to use scotch tape to tape the adjacent faces together after gluing while waiting for the glue to set. Also strong alligator clips are useful in holding the glued tabs together while the glue sets up. Have fun and may the glue be with you.

Once you have several virus capsid models constructed, you will observe numerous closed rings of protein molecules (clumps) as illustrated in Figure 10 or as directly visible in the plant virus capsids illustrated in Figure 11. These closed periodically spaced protein clump rings form a pathway for mechanical wave motion. In fact they are a biological manifestation of the classical physics problem of wave motion on a periodically spaced mass beads on an elastic string with circular boundary conditions. The solutions to the problem are the well known quantatized standing wave solutions. For each quantatized wavelength solution there are two transverse oscillation modes for the system (closed ring) and one longitudinal oscillation mode. There is a total number of independent oscillation modes equal to three times the number of masses in the closed ring. Looking at Figure 10, one transverse mode would be protein molecules (clumps) being alternately displaced above and below the plane of the page. The other transverse oscillation mode for the same particular wavelength solution would be at right angles to this other mode. It would consist of the alternate displacement of the same protein clumps toward and away from the center of the closed ring of protein clumps. The longitudinal mode consists of protein clumps being displaced back and forth about their equilibrium position along the arc length of the ring. All three modes are allowed to exist simultaneously. Figure 12A shows a mathematical abstraction of a closed ring of ten protein molecules (clumps). Figure 12B shows the same ring linearized and extended in length for graphical purposes to easily illustrate standing wave motion. Figures 12C,D, and E, show the transverse and or longitudinal displacement patterns associated with some of the standing wave solutions for the ring. Similar displacement patterns can be drawn for other closed rings with various numbers of protein clumps per ring. For example Figure 12 F and G illustrate the standing wave pattern for a ring consisting of five protein molecules. What is crucial to note is that some standing wave displacement patterns put far more stress on the ring than others. The most stressful standing wave displacement pattern is one where adjacent protein molecules (clumps) oscillate 180 degrees out of phase as illustrated in Figure 12C. This mode places maximum stress on the relatively weak adjoining bonds between these protein clumps. If the displacement amplitude becomes to large the bonds will rupture and the ring will disintegrate. Now

examining the various capsid models you have constructed, you will note these ring patterns are commonly overlapping and or tangentially bonded to each other. For example the capsid constructed from Figure 9C has how many: 1) Rings with five member protein clumps, 2) Rings with six member protein clumps, 3) Rings with ten member protein clumps, and 4) Rings with fifteen member protein clumps? How many of the five member rings overlap with each other? How many of the five member rings are tangential to each other? With how many other six member rings does each six member ring overlap or intersect? With how many other ten member rings does each ten member ring overlap or intersect? With how many other fifteen member rings does each fifteen member ring overlap or intersect? Now how do all of the rings overlap or intersect with each other? By now you should have had a cathartic experience realizing just how cross coupled even a very simple virus capsid is when considered as a reservoir for standing wave energy. Now realize that at each overlap or intersection region for each protein molecule in the rings discussed above, the bond strength is relatively very weak and that combined random mixing of standing wave displacement amplitudes from even ultra low intensity ($\sim 10^{-16}$ w/m^2) standing waves on the various rings can rupture these bonding regions. When Rife exposed viruses to their most stressful mechanical oscillation mode, he could literally while viewing them through his microscope, see them disintegrate and or even explode. And as was shown in Appendix B, Rife was only using ultrasound intensity levels of around 10^{-16} w/m^2 .

So far we have avoided the use of mathematics and differential equations to illustrate standing wave motion on the virus protein coat (capsid). However, to fully appreciate how and why a virus is so susceptible to its own mechanical structural resonant vibration frequency it is necessary to apply some simple physics to the problem. All the physics that will be used is readily available in undergraduate physics mechanics text books, so I will simply state the results here. Figure 13A illustrates a ten member protein clump ring such as we have found in virus capsids. Figure 13B is the mathematical abstraction of Figure 13A. Figure 13C focuses in on the oscillation of a single protein clump of the ring while it is executing a single mode oscillation of the most stressful oscillation mode to bonds in the ring. (The results we will obtain are however valid for all oscillation modes.) The differential equation of motion for free oscillation of the system shown in Figure 13C is equation 1.

$$d^2S/dt^2 + (b/m) dS/dt + W_0^2 S = 0 , \qquad \text{Equation 1}$$

where S is displacement of the center of mass from its equilibrium position, m is the mass of the protein molecule, b is a positive drag factor constant, and W_0 is the natural resonance angular frequency of the system. If the mass m of the system is displaced a distance So from its equilibrium position and then released to perform free oscillation* , a situation as depicted in Figure 14 will then occur. This is the graphical representation of the solution to equation 1. Figure 14 shows that the amplitude of oscillation decreases exponentially with time due to the velocity dependent drag force. The strength of the drag force is represented by the magnitude of b. A useful quantity when discussing oscillating mass systems is the Q-value defined as:

$$Q = (W_0 m)/b , \qquad \text{Equation 2.}$$

* For the ring as a whole this corresponds to each protein molecule initially being displaced a distance So from its equilibrium, with adjacent molecules being displaced in opposite directions and then being released to freely oscillate.

FIGURE 11

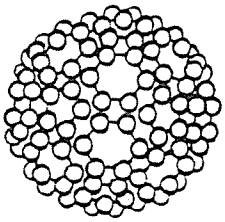

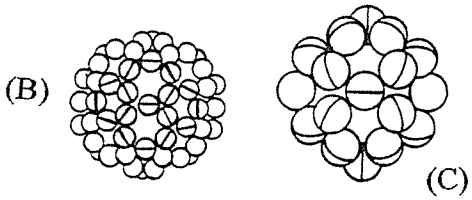

(A) TURNIP YELLOWS MOSAIC VIRUS
(B) TURNIP CRINKLE VIRUS
(C) SMALL TURNIP CRINKLE VIRUS

FIGURE 13

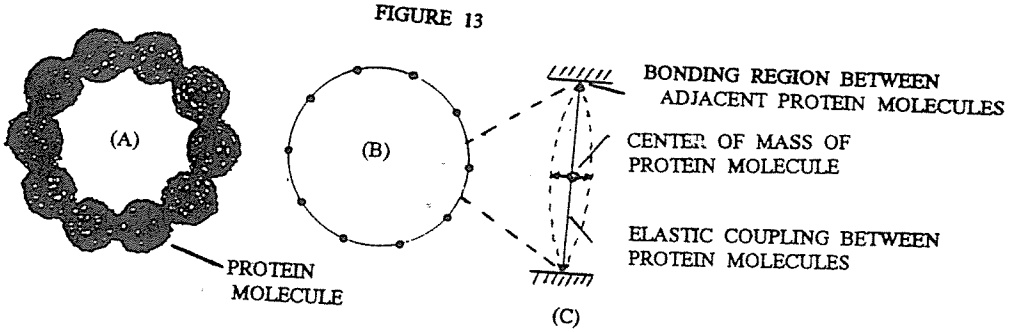

FIGURE 12

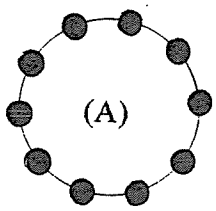

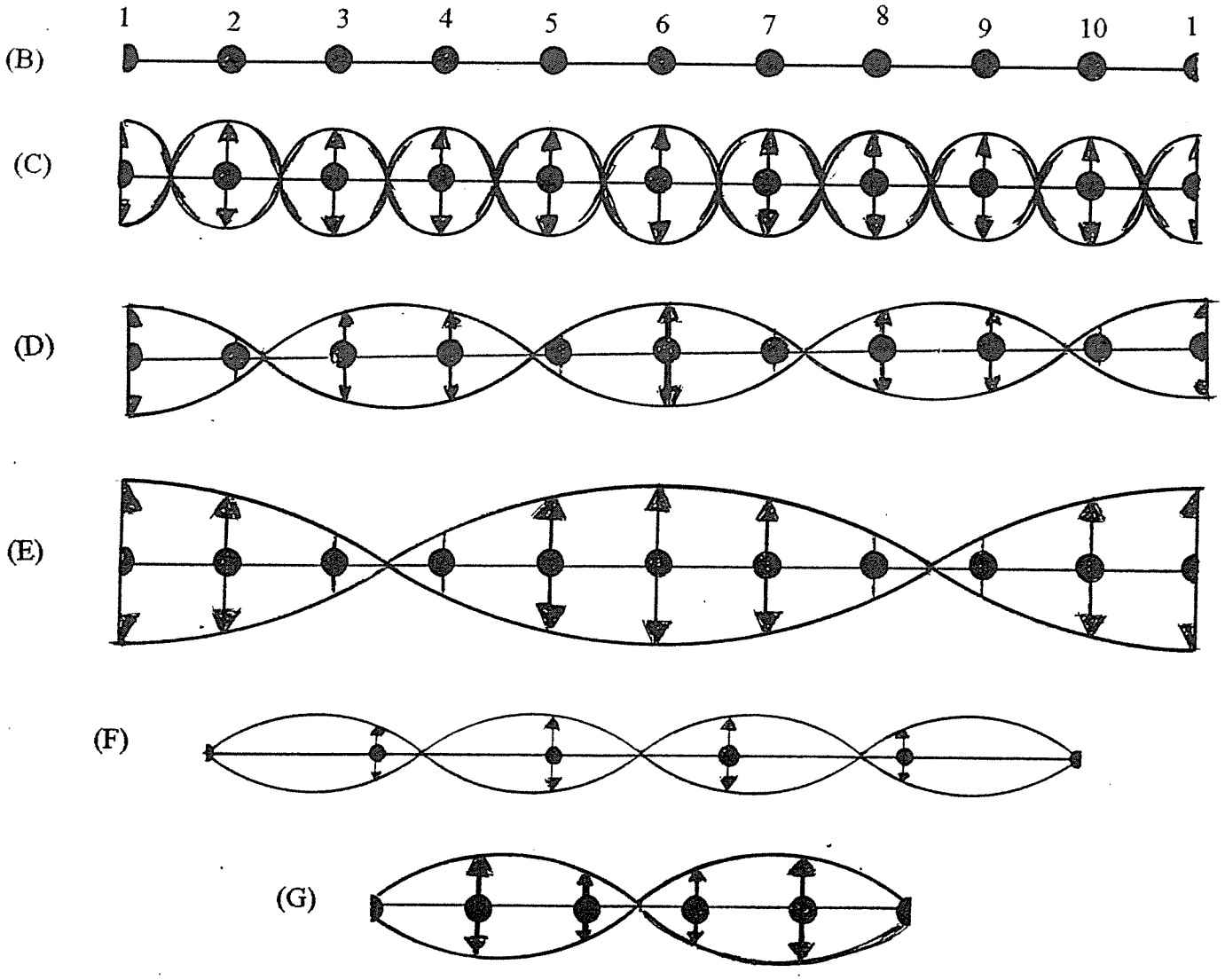

When the Q-value is large (relatively small b) , as it is for the oscillating mass system depicted in Figure 14, then the average power (P_d) radiated or dissipated by the oscillating system per oscillation cycle is given approximately by:

$$P_d = E(W_o/Q) , \qquad \text{Equation 3,}$$

where E is the total energy of the oscillating system at the time of interest. For our system almost all power is dissipated in the form of pressure waves in the fluid medium in which the virus is maintained.

Now if the system in Figure 13C were to be exposed to a periodic driving force such as sinusoidal pressure waves, then the differential equation of motion for the system would be given by:

$$d^2S/dt^2 + (b/m)\, dS/dt + W_o^2\, S = F_o \operatorname{Sin} Wt , \qquad \text{Equation 4,}$$

where F_o is a constant and the maximum amplitude of the driving force (F_o Sin Wt). The steady state solution to equation 4 is:

$$S = B \operatorname{Cos} (Wt - \&) , \qquad \text{Equation 5,}$$

where & is a phase constant and B is given by :

$$B = (F_o)/(m^2(W_o^2 - W^2)^2 + W^2 b^2)^{1/2} , \qquad \text{Equation 6.}$$

Figure 15 shows B plotted against the angular frequency of the driving force for the case where the mass and the peak value of the driving force are held constant while the drag force is allowed to vary. Note the horizontal dashed line that intercepts the curve for $b = b_o$. Let the displacement value (oscillation amplitude) given where the dashed line intercepts the displacement axis be the displacement value which corresponds to the oscillator self distruction (adjacent protein bonds rupture). In this situation Figure 15 would then indicate that for the driving force used, the protein ring would be ruptured, if b was much smaller then $3b_o$. Another way to say this is , if your oscillator has a very small b value, then a very small driving force can destroy it provided the driving frequency is close enough to the resonance frequency.

Still another approach to understanding the oscillator self distruction process is to look at the power absorption by the oscillator from the driving force. Equation 7 gives the power absorption (P_a) of the oscillator from the driving force.

$$P_a = (1/2\, F_o W^2 b) / (m^2(W^2 - W_o^2)^2 + W^2 b^2) , \qquad \text{Equation 7.}$$

Pa is plotted verses angular frequency in Figure 16 for a constant value of maximum driving force F_o , constant mass (m), and three values of b. The curve in Figure 16 are for a situation of dynamic equilibrium. That is power absorption from the driving force equals power being dissipated by the oscillator. In our case almost all dissipation is done by re-radiation of the pressure wave, which is driving the system. Let the dashed line intercept indicate the re-radiation power level at which the oscillator's amplitude is at the

FIGURE 14

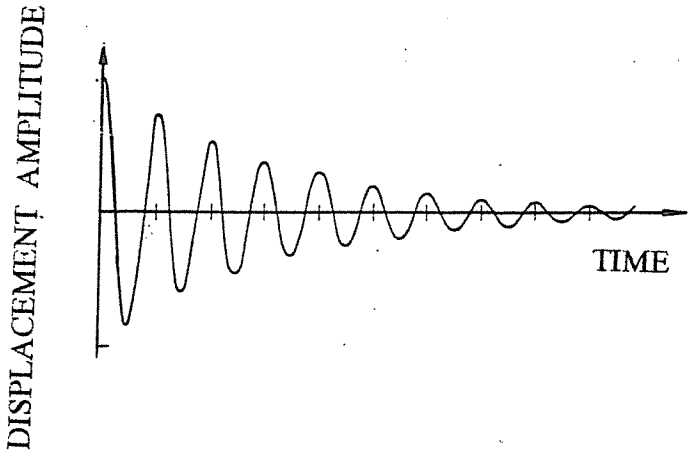

FIGURE 15

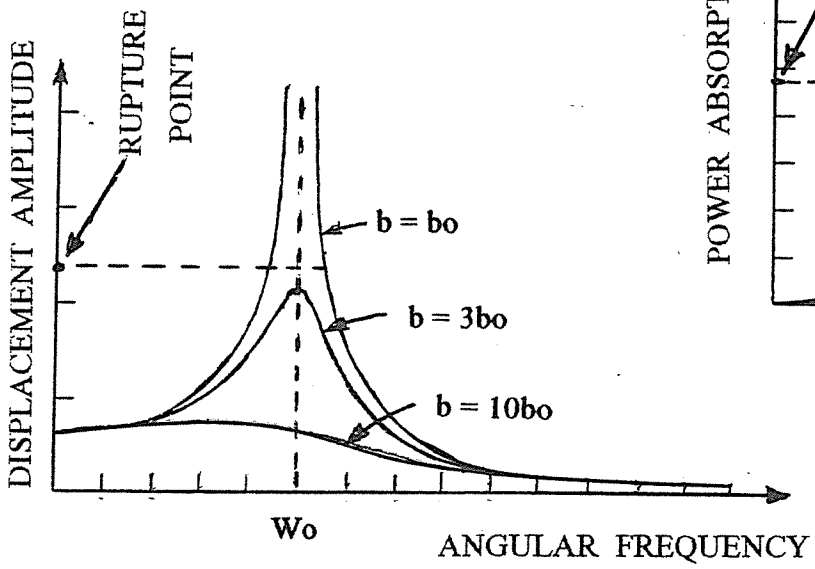

FIGURE 16

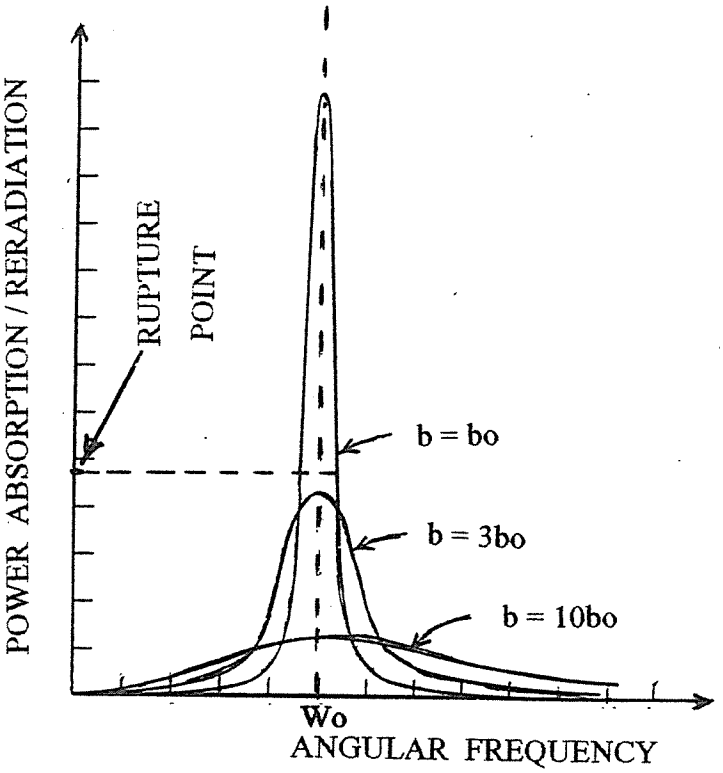

FIGURE 17

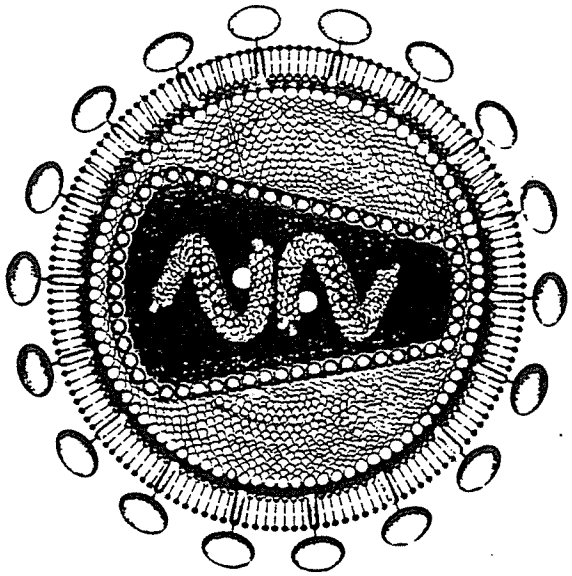

Approximately half the re-radiated ultrasound is emitted to the interior of the virus capsid. If the interior re-radiated ultrasound has a frequency near one of the main resonant structural vibration frequency, it will be readily re-absorbed by the capsid. This has the effect of effectively increasing the Q-value of the individual oscillators in the protein rings, over that of the isolated ring. The effect of all of this is that the curves in Figures 15 and 16 for actual viruses should be even sharper (the same protein rings in viruses are easier to destroy by structural resonant vibrations).

self destruct point. Any further power absorption and the oscillator will not be able to increase its amplitude of oscillation because it will come apart (rupture). Figure 16 illustrates that if your oscillator has a small enough b value, then a very small driving force can destroy it, provided the driving frequency is close enough to the resonance frequency (W_O).

Let us now return our attention to viruses with helical symmetry. Close examination of the two prototype helical viruses of Figures 1 and 2 shows that what we have in these two viruses is a good analog to an elastic spring. And just like an elastic spring you will have a natural specific torsional resonance frequency for each helical virus. For example for a torsional spring oscillation, the equation of motion is given by:

$$(I)dS^2/dt^2 = - CS, \qquad \text{Equation 8}$$

where I is the moment of inertia of the helical mass about its length axis, S is the angular displacement from equilibrium (zero torque), and C is the torsional stiffness , a constant. Equation 8 has a solution of:

$$W_O = (C/I)^{1/2} \quad , \qquad \text{Equation 9.}$$

If this frequency of ultrasound is applied to the helical structure with enough intensity the helix will come apart. It should also be noted that relatively long (large length to width ratio) helical viruses should also be susceptible to damage by ultrasound frequencies that set up standing longitudinal wave motion along the virus axis. And particularly the simultaneous application of ultrasound frequencies for both torsional and longitudinal standing waves should be particularly destructive to the helical viruses. With the proper choice of frequencies and relative intensity between frequencies and absolute intensities we should be able to convert helical viruses into organic trash in one second or so.

Before taking up bacterial susceptibility to structural resonant vibrations, let us summarize what has been learned about destroying and or controlling virus infections using structural resonant vibrations. Figure 17 illustrates the structure of the supposed cause of AIDS, the HIV. HIV has three obvious periodic structures that can be attacked by structural resonant vibrations. First, there are the periodically placed glycoprotein spikes on the surface. Second, there is the deltahedra outer capsid. Third, there is the inner capsid. Each of these structures is destructible by its own structural resonant vibrations. Since the ultrasound intensity levels of structural resonant vibrations required to destroy a virus are so ultra low (10^{-16} w/m^2) , it is practical to keep a person infected with a virus under continuous exposure to structural resonant vibrations for that virus. This can be achieved in several ways: 1) The person can ware a small inconspicuous ultrasound transducer unit (see Appendix F), 2) Rife frequency instrument type "light" can be installed at home or in the work place, and 3) Structural resonant vibration ultrasound can be carried by the room air. Now, if the body's immune system is actively hunting for and destroying cells infected with the virus of interest (this process can be stimulated by a vaccine) and if the virus is not being allowed to infect new cells do to its destruction by structural resonant vibrations, then the body can potentially rid its self of the virus completely.

Now on to bacteria destruction by structural resonant vibrations. From the remnants of Rife's work still publicly available, it is clear that Rife was able to destroy all bacteria he encountered using his frequency instrument. In other words he could just as easily destroy viruses as bacteria with his frequency instrument (see Appendix B) . It is assumed in the first sentence of this paragraph that bacteria can be destroyed by structural resonant vibration phenomenon, which are of the same nature as that for virus distruction. I know of no direct observational proof of that. However, there is good circumstantial evidence for it. Though the cell wall structure of bacteria in general appears to be a continuous strong tough uniform material, a closer look at high power with electron microscopes show that there are numerous pores, surface projections, such as pili, which are transmembrane and transwall structures as are flagella. All of these structures have periodic protein clump structures associated with there construction and or immediate environment. For example, pili protein subunits(clumps) are arranged in a regular helical configuration. Which, if any of the above periodic protein clump structures can be easily disrupted by structural resonant vibrations is not known at present. Someone or some institution will need to construct a modernized version of a Rife microscope (see Appendix A) and actually observe bacteria cell distruction by a Rife frequency instrument device to determine where the weak spots are in the bacteria cell wall which allow osmotic pressure to rupture the bacteria and spill its contents out.

You should now understand how Rife, using his frequency instrument, was able by 1939 to destroy the viral and bacterial pathogens associated with 52 major diseases, including cancer (see Appendix G for connection between BX and BY cancer viruses and the genetics of cancer cells). Rife's results were fully and completely verified by the 1934, 1935, and 1937 test clinical trials, which were carried out by the U.S.C. Medical School Special Medical Research Committee, that oversaw the clinical trials. The responsibility for the deaths of, suffering by, and the financial ruin of tens upon tens of millions of people since 1937 clearly rests with the cowardly, greedy, and corrupt leadership/ownership of the medical industry. This includes pharmaceutical and insurance companies which have been major benefactors and pervaors of the greed and associated corruption. Rife treatment methods should be available everywhere right now! Of coarse this would reduce patient suffering and so called health costs in the U.S. by 50% or more. Now who do you think will resist Rife treatment implementation? Who do you think will attempt to and has had laws like the Weinberger law in California passed so that you can only be treated for cancer by a allopathic medical doctor that only can use: 1) Surgery, 2) Radiation, and or 3) Chemotherapy?

In China doctors are paid only when the people in their practice remain healthy or are made well. We need to adopt a strong value given for value received attitude when dealing with allopathic doctors. Of coarse we must insist that these doctors go back to school and learn what health is and its relationship to good nutrition, mega-nutrition, diet, exercise, and emotional health. We must also insist that cheap effective treatment methods, drugs, and remedies, which have been suppressed for over 10, 20, 30, 40, 50 plus years now by vested monopolistic interests be made readily available at affordable prices (see Appendix H for examples of very effective suppressed cheap remedies).

Taken from: DR.RIFE AND THE DEATH OF THE CANCER INDUSTRY,
a paper by physicist Gary Wade 7/13/93
For info write: Gary Wade, ~~P.O. BOX 3015, Alhambra, CA. 91803~~